Molecular Microbiology (2006) **62**(6), 1631–1642
doi:10.1111/j.1365-2958.2006.05485.x
First published online 13 November 2006

Dimeric structure of the cell shape protein MreC and its functional implications

Fusinita van den Ent,[1]* Mark Leaver,[2] Felipe Bendezu,[3] Jeff Errington,[2] Piet de Boer[3] and Jan Löwe[1]
[1]*MRC-LMB, Hills Road, Cambridge CB2 2QH, UK.*
[2]*Institute for Cell and Molecular Biosciences, Newcastle University, Newcastle-upon-Tyne NE2 4HH, UK.*
[3]*Department of Molecular Biology and Microbiology, Case Western Reserve University, Cleveland, OH 44106-4960, USA.*

Summary

The bacterial actin homologue MreB forms helical filaments in the cytoplasm of rod-shaped bacteria where it helps maintain the shape of the cell. *MreB* is co-transcribed with *mreC* that encodes a bitopic membrane protein with a major periplasmic domain. Like MreB, MreC is localized in a helical pattern and might be involved in the spatial organization of the peptidoglycan synthesis machinery. Here, we present the structure of the major, periplasmic part of MreC from *Listeria monocytogenes* at 2.5 Å resolution. MreC forms a dimer through an intimate contact along an N-terminal α-helix that connects the transmembrane region with two C-terminal β-domains. The translational relationship between the molecules enables, in principle, filament formation. One of the β-domains shows structural similarity to the chymotrypsin family of proteins and possesses a highly conserved Thr Ser dipeptide. Unexpectedly, mutagenesis studies show that the dipeptide is dispensable for maintaining cell shape and viability in both *Escherichia coli* and *Bacillus subtilis*. Bacterial two-hybrid experiments reveal that MreC interacts with high-molecular-weight penicillin-binding proteins (PBPs), rather than with low-molecular-weight endo- and carboxypeptidases, indicating that MreC might act as a scaffold to which the murein synthases are recruited in order to spatially organize the synthesis of new cell wall material. Deletion analyses indicate which domains of *B. subtilis* MreC are required for interaction with MreD as well as with the PBPs.

Accepted 17 October, 2006. *For correspondence. E-mail fent@mrc-lmb.cam.ac.uk; Tel. (+44) 122 325 2969; Fax (+44) 122 321 3556.

Introduction

The majority of bacteria have a rigid cell wall that maintains their cell shape and resists internal turgor pressure. A fine network of glycan strands linked together by short peptides forms a peptidoglycan (PG) layer (or murein sacculus) that is responsible for the rigidity of the bacterial cell wall (reviewed in Bhavsar and Brown, 2006). As isolated murein sacculi retain the shape of the cell from which they are derived, it is thought that the information for cell shape is implemented in the sacculus (Höltje, 1998). Indeed, many mutations that affect cell shape are located in genes involved in PG synthesis (Spratt, 1975; Spratt and Pardee, 1975; Tamaki *et al*., 1980; Henriques *et al*., 1998; Nelson and Young, 2000; Wei *et al*., 2003; Nilsen *et al*., 2004). The PG layer is assembled from precursors by a family of proteins known as penicillin-binding proteins (PBPs) that form and cross-link glycan strands through their glycosyl transferase and transpeptidase activities (Höltje, 1998; Popham and Young, 2003). Murein hydrolases create gaps in the PG layer, and in Gram-negative organisms it is thought that newly synthesized peptidoglycan strands are inserted into these gaps to enable cell elongation and septation to occur (Heidrich *et al*., 2002).

In order to maintain the shape of the cell, the PBPs as well as the murein hydrolases are likely to be temporally and spatially organized. It has been speculated that some of the proteins that affect cell morphology, such as MreB, MreC and MreD (encoded by the *mreBCD* operon), might position the peptidoglycan synthesis machinery, while others, such as RodA and FtsW, might be involved in transport of PG precursors (Tamaki *et al*., 1980; Wachi *et al*., 1987; Levin *et al*., 1992; Varley and Stewart, 1992; Henriques *et al*., 1998; Jones *et al*., 2001; Lee and Stewart, 2003; Figge *et al*., 2004; Gitai *et al*., 2004; Formstone and Errington, 2005; Kruse *et al*., 2005; Leaver and Errington, 2005).

Depletion of MreB, MreC or MreD showed that they are essential for viability and maintenance of the natural shape of the bacterial cell (Lee and Stewart, 2003; Soufo and Graumann, 2003; Formstone and Errington, 2005; Kruse *et al*., 2005). The *mre* (for murein region 'e') genes were initially identified in *Escherichia coli* mutants that were affected in their sensitivity to mecillinam, an antibiotic known to inhibit PBP2 (Wachi *et al*., 1987; 1989).

MreB forms cytoskeletal filaments that follow a helical path just underneath the cell membrane (Jones *et al*., 2001; Kruse *et al*., 2003; Defeu Soufo and Graumann, 2004; Figge *et al*., 2004; Gitai *et al*., 2004; Kruse and Gerdes, 2005). The structure of MreB resembles that of actin (van den Ent *et al*., 2001) and the polymer is reminiscent of the one strand of filamentous actin (Amos *et al*., 2004; Löwe *et al*., 2004), indicating that an actin-like cytoskeleton in bacteria is required for cell shape determination. *Bacillus subtilis* has two additional MreB-like genes, Mbl and MreBH, which are now thought to colocalize and therefore to form a single helical cable system (Jones *et al*., 2001; Carballido-Lopez and Errington, 2003; Carballido-Lopez *et al*., 2006; Defeu Soufo and Graumann, 2004). All three isologues affect morphogenesis of the cylindrical part of the cell wall (Jones *et al*., 2001; Soufo and Graumann, 2003), suggesting that they all participate, directly or indirectly, in organization of the wall synthetic system. Using fluorescently labelled vancomycin (that binds the D-ala-D-ala ends of nascent peptidoglycan subunits before they are cross-linked to peptides), it has been shown that new peptidoglycan in *B. subtilis* is incorporated into the pre-existing cell wall in a helical pattern that is reminiscent of and influenced by the MreB/Mbl/MreBH cables (Daniel and Errington, 2003; Tiyanont *et al*., 2006). PBP2, involved in longitudinal growth of the peptidoglycan in *Caulobacter crescentus*, exhibits a helical pattern similar to that of MreB (Figge *et al*., 2004), further supporting a link between the Mre proteins and the PG-synthesizing machinery. Apart from directing cell shape, the MreB cytoskeleton might also be involved in other functions, such as chromosome partitioning (Soufo and Graumann, 2003; Gitai *et al*., 2005; Kruse *et al*., 2006).

The widely conserved genes *mreC* and *mreD* are usually arranged immediately downstream of *mreB* (Wachi *et al*., 1989; Levin *et al*., 1992; Varley and Stewart, 1992) in the same operon (Formstone and Errington, 2005) and are associated with the membrane and the division site (Lee *et al*., 2003; Leaver and Errington, 2005). In contrast to the polytopic membrane protein MreD, MreC is predicted to have a single transmembrane spanning helix with the major C-terminal domain located in the periplasm. Indeed, fractionation studies have shown that MreC is associated with the inner membrane (Kruse *et al*., 2003). Topology experiments using a PhoA fusion to MreC have indicated that the major C-terminal part is located in the periplasm, whereas the N-terminal helix anchors the protein in the membrane (Lee *et al*., 2003).

Depletion of MreC or MreD results in the formation of spherical cells that eventually lyse, possibly because of a deficiency in peptidoglycan synthesis in the cylindrical part of the cell (Lee and Stewart, 2003; Leaver and Errington, 2005). MreC in *C. crescentus* interacts with several PBPs (Divakaruni *et al*., 2005) and colocalizes with PBP2 in *Rhodobacter sphaeroides* (Slovak *et al*., 2006). PBP2 forms helical structures that depend on MreB (Figge *et al*., 2004). Also, MreC has been found to localize in a helical fashion (Dye *et al*., 2005; Leaver and Errington, 2005), suggesting that it might form a bridge between the intracellular cytoskeleton and the periplasmic cell wall synthesis machinery. An indication that MreC does interact with the cytoskeleton has come from bacterial two-hybrid screens in *E. coli*, where MreC might interact with MreB as well as MreD (Kruse *et al*., 2005). In addition, the helical organization of the MreB cytoskeleton in *E. coli* is dependent on the presence of MreC, again suggesting a link between MreB and MreC (Kruse *et al*., 2005). Recently, it has been shown that in *C. crescentus* MreB and MreC might localize independently of each other, whereas the localization of PBP2 depends on both of them (Dye *et al*., 2005).

Here, we present the crystal structure of the major, periplasmic part of MreC from *Listeria monocytogenes* at 2.5 Å resolution. MreC forms a dimer through an intimate contact along the N-terminal α-helix that connects the transmembrane region with the C-terminal β-domains. The second β-domain has structural similarity to the chymotrypsin family of proteins and possesses highly conserved Thr and Ser residues (TS dipeptide). To investigate whether these residues are important for MreC function, they were mutated in *E. coli* and *B. subtilis*. Despite their high degree of conservation these residues are not essential for viability and maintenance of cell shape. Bacterial two-hybrid studies revealed that MreC interacts with the high-molecular-weight murein synthases rather than with the low-molecular-weight peptidases and deletion analyses indicate the domains of *B. subtilis* MreC that are required for interaction with MreD and several of the PBPs.

Results and discussion

Crystal structure of MreC

The crystal structure of the periplasmic part of MreC from the Gram-positive bacterium *L. monocytogenes* reveals two β-strand domains arranged as wings of a butterfly around a central, N-terminal helix (Fig. 1A). Following the N-terminal helix, the first wing encompasses two β-sheets in an orthogonal arrangement, each consisting of three antiparallel β-strands. The second wing is inserted in front of the C-terminal β-strand of the first wing and contains six antiparallel β-strands, wrapped around each other as in the canonical β-barrel fold. The crystal structure shows MreC in close dimeric contact through a long N-terminal helix (Fig. 1B) as well as through its globular domains (Fig. 4). The helices are

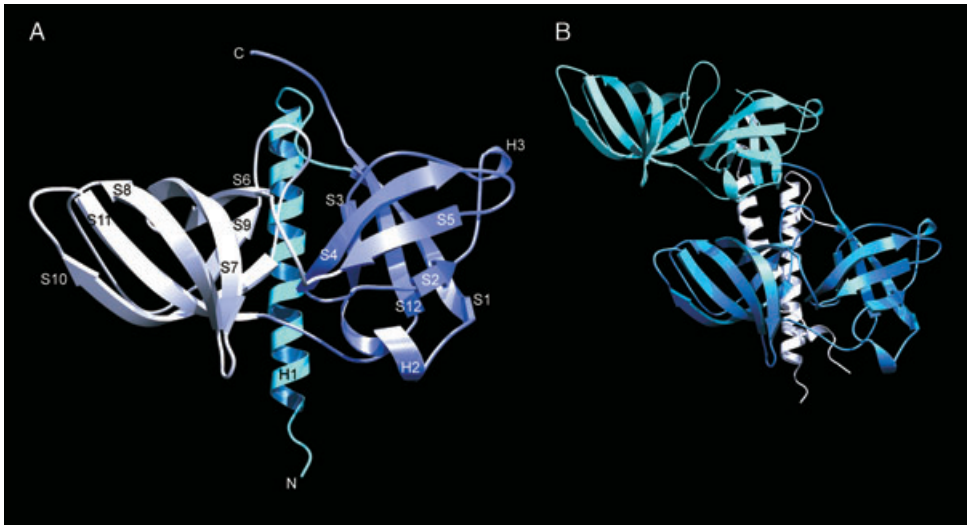

Fig. 1. A. Ribbon plot of the crystal structure of the major, periplasmic part of MreC (aa 74–283) from *L. monocytogenes* at 2.5 Å resolution. The secondary structure elements are labelled according to their appearance in the primary sequence.
B. MreC dimerizes through its extended N-terminal helix (in white). The second molecule (depicted in cyan) is a simple translation of the first molecule (blue).
Figures were prepared using MOLSCRIPT and RASTER3D (Kraulis, 1991; Merritt and Bacon, 1997).

held together via hydrophobic interactions between leucine residues, some of them participating in a hepta repeat typical of leucine zippers (Figs 1B and 3). The β-domains of the second molecule are simply translated along the longitudinal axis of the coiled coil domain. This has the implication that the surface of the dimer interface in the β-domain belonging to one molecule is solvent exposed in the other molecule. In principle this could enable filament formation, resulting in a step-like chain of alternating first and second β-domains, with the pairs of helices protruding from every second molecule. The helices point in a similar direction that favours anchoring of both N-termini in the cytoplasmic membrane. A major part of the dimeric interface is dependent on the extended helices, which have a buried surface of 1892 Å^2 at the interface, whereas the globular domains have a buried surface 1304 Å^2. It needs to be established whether the latter is enough to exert filament formation or whether additional interactions may be needed to support this kind of arrangement.

A similarity search among the currently known structures in the protein databank shows that the first β-domain of MreC has structural similarity with a small nucleolar RNP similar to Gar-1 (Rashid *et al.*, 2006). The second β-domain of MreC is similar to the β-barrel fold characteristic of the family of Trypsin-like serine proteases, of which two of the most similar structures to MreC are shown in Fig. 2 (α-lytic protease and the serine protease SPL). Encouraged by this finding, we investigated whether MreC would have any of the residues that make up the catalytic triad in this family of proteases. The triad of α-lytic protease (Fuhrmann *et al.*, 2004) consists of Asp102, His57 and Ser195, where Ser195 (depicted in yellow in Fig. 2) is the primary nucleophile. Sequence analysis of over 30 bacterial genomes revealed that MreC contains highly conserved Ser and Thr residues (TS dipeptide) (Fig. 3). These residues are located in the second β-domain, in a loop connecting strand 9 and 10 (shown in red in Fig. 2). Superposition of the second β-domain of MreC on the two proteases shows that the conserved Ser of MreC overlaps with a Ser in both proteases (shown in red in Fig. 2). However, the Ser residues in the proteases are not part of the active site, making it unlikely that the conserved dipeptide in MreC is involved in a Trypsin-like protease activity.

The degree of conservation of all residues was calculated based on an alignment of over 30 different *mreC* genes and was mapped onto the surface of the structure of the MreC dimer (Fig. 4). The conserved Ser226 is located at the bottom of a channel accessible from the front of the molecule (see arrow in Fig. 4A). At the back of the molecule, access to the cleft containing these conserved residues (arrow in Fig. 4B) is hampered by the N-terminal helices, involved in dimer formation. The N-terminal helix of the second molecule interacts with that of the first molecule and hence the cleft with the conserved Ser and Thr residues in the second molecule remains accessible upon dimer formation.

The conservation plot also shows that the conserved stretch of amino acids (in red) at either end of the N-terminal helix in one molecule makes contact with the similar region in the other molecule, supporting that dimer formation as observed in the crystal structure is

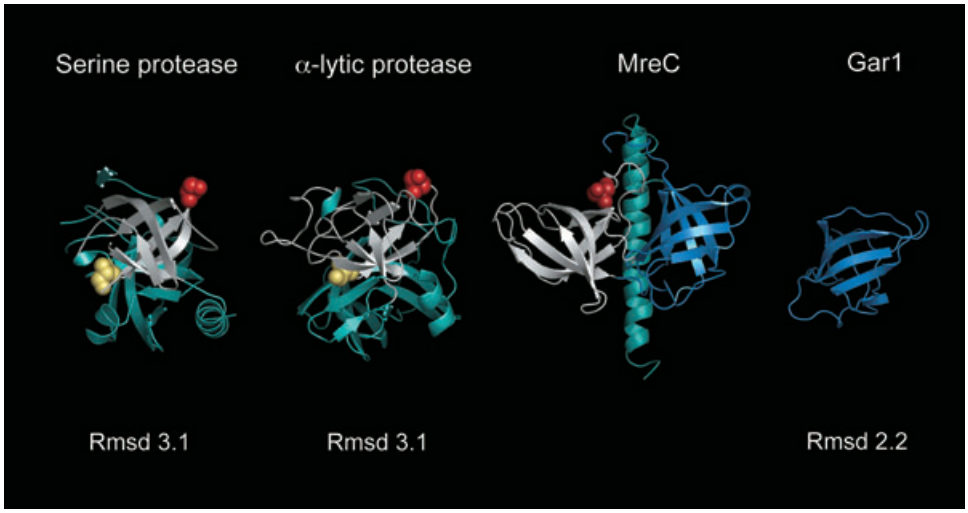

Fig. 2. Three top scores of a structural similarity search with MreC among all known structures in the PDB (using DALI; Holm and Sander, 1993). The first β-domain of MreC (depicted in blue) has structural resemblance to a small nucleolar RNP similar to Gar-1 [PDP entry 2ey4-c, *Z*-score 7.2, root mean square deviation (Rmsd) of superimposed 64 CA atoms of 2.2 Å]. The second β-domain of MreC (depicted in white) has structural similarity to α-lytic protease (PDB entry 1qq4, *Z*-score 7.3, Rmsd 3.2 Å over 85 residues) and the serine protease SPL from *Staphylococcus aureus* (PDB entry 2as9, *Z*-score 6.7, Rmsd 3.1 Å over 68 residues). Colour codes: blue domains show structural similarity to each other as do the white domains, structural elements depicted in cyan are distinct. Conserved Ser 226 in MreC is depicted in red and superimposes on the red Ser residues in the proteases, whose active sites are depicted in yellow. The figure was prepared using PYMOL (DeLano, 2002).

functionally relevant (Fig. 4B). Size-exclusion chromatography suggests that the periplasmic portion of MreC from *E. coli*, *B. subtilis* and *L. monocytogenes* all form a dimer in solution at a concentration of 3 mg ml^{-1} (data not shown). As discussed below, two-hybrid studies also show that *B. subtilis* MreC self-interacts, supporting dimer formation in a more physiological context.

Mutational analysis of MreC in vivo

To investigate whether the conserved diad Thr225 and Ser226 is required for MreC function, the corresponding residues in *B. subtilis* and *E. coli* MreC were changed to Ala Ala, and the phenotypes of the mutant alleles were determined. Because *mreC* is essential, a *B. subtilis* strain (P_{xyl}-*mreC*) expressing an ectopic copy of native *mreC* under the control of an inducible promoter was constructed. Subsequently, the original copy was either deleted (Δ*mreC*, strain 3461) or mutated (strain 3473), and cells were grown in the absence of xylose to reveal the phenotype of the mutations. In contrast to the complete deletion mutant of *mreC*, changing the conserved Ser and Thr residues into alanines did neither affect cell shape nor affect cell viability (Fig. 5A). To confirm that the mutation was not lethal, the *mreC*^{TS230AA} allele was introduced in a wild-type background. The resulting strain (3474) did not show any shape defects and grew as wild type.

Surprised by the finding that these highly conserved residues are clearly not essential for MreC function in *B. subtilis*, the comparable mutations were introduced in *mreC* of *E. coli*, which lacks the extra MreB-like genes of *B. subtilis*. To this end, the double mutant (T222A,S223A) was introduced in MreC fused to RFP (cherry) and tested for its ability to convert the spherical shape of Δ*mreC* cells back to rods. Briefly, plasmids pFB211[P_{lac}*::mreC-rfp*], pFB218[P_{lac}*::mreC(T222A,S223A)-rfp*], pFB223[P_{lac}*::mreC(1–104)-rfp*] and a vector control (pMLB1113) were transformed into the Δ*mreC* strain FB15/pFB112/pFB128[Δ*mreC/sdiA/cI857* $P_{\lambda R}$*::mreD*] and cells were grown at 37°C in LB in the presence of IPTG (a range from 0 to 250 μM) to induce expression of the *mreC* fusions. Transformants carrying pFB211 or pFB218 underwent shape conversion from sphere to rod in an IPTG-dependent manner (10 μM, or higher), while those carrying pFB223 or pMLB1113 remained spherical (even at 250 μM inducer). RFP fused to the wild-type as well as the double mutant protein correctly localized peripherally (Kruse *et al*., 2005). Thus, whereas MreC(1–104) was insufficient for function, the MreC(T222A,S223A)–RFP fusion appeared to be fully functional.

Based on the above findings, it is very unlikely that these conserved residues are part of an active site. The high degree of conservation of Thr225 might be explained by its structural role. Thr225 is located at the end of β-strand S9 where it interacts with a moderately conserved Gly235. Similarly, Gly227 flanking Ser226 interacts with a conserved Pro233 in the loop connecting S9 with S10. However, the reason for the presence of the highly conserved Ser226 is not so

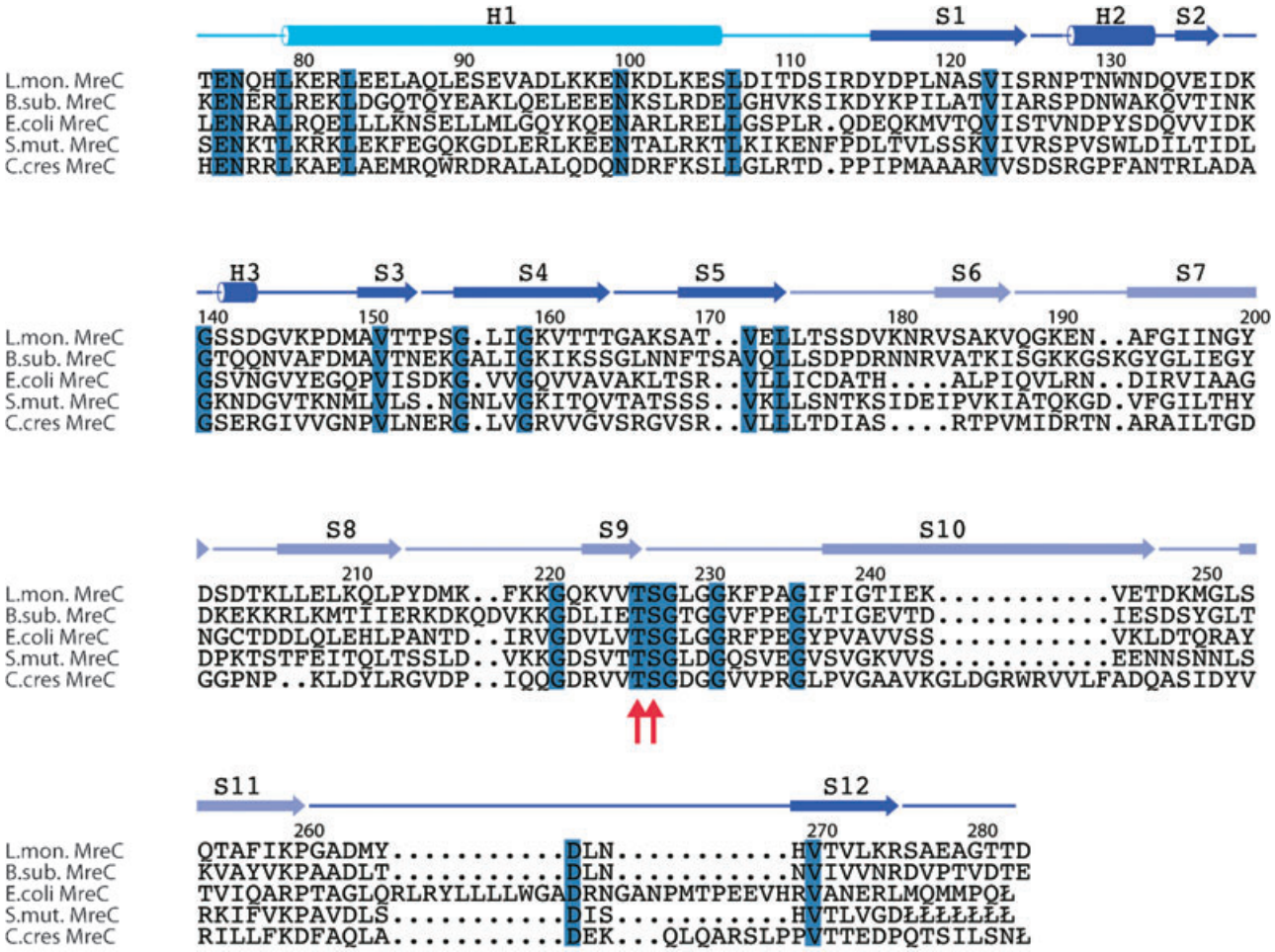

Fig. 3. Sequence alignment of MreC from *L. monocytogenes*, *B. subtilis*, *E. coli*, *Streptococcus mutans* and *C. crescentus* with the secondary structure elements of *L. monocytogenes* MreC depicted on top (cylinders for α-helices and arrows for β-strands). The blue coloured residues are conserved among the five sequences shown. The red arrows point towards two absolutely conserved residues among 30 MreC sequences. Numbers are relative to the *L. monocytogenes* MreC sequence. The figure was prepared using ALSCRIPT (Barton, 1993).

obvious. It might be involved in interactions with a binding partner or has some other function that is redundant and therefore not detectable in the *in vivo* assays described above.

Interaction partners for MreC

Both the crystal structure and size exclusion chromatography prove MreC to be a dimer. To test for dimerization *in vivo* we turned to the bacterial two-hybrid system of Karimova *et al*. (1998). Full-length copies of MreC (MreC1-290) did indeed interact strongly, consistent with dimer formation *in vivo* (Fig. 6). A C-terminal deletion mutant lacking the two β-domains (MreC1–113) was still able to interact with full-length MreC, whereas further truncations of the N-terminal periplasmic helix H1 (MreC1–77, 1–41, 1–25) eliminated a detectable interaction. This would be consistent with the crystal structure, in which dimerization occurs via intertwining of the extended N-terminal helices of the monomers.

Full-length, dimeric MreC also interacted strongly with integral membrane protein MreD (Fig. 6). However, this interaction was lost in all of the truncated constructs, suggesting that a more extensive segment of MreC, including at least part of the β-domain region, is needed for MreC–MreD interaction.

Previously, it has been shown that the phenotype of cells doubly mutated for *pbpH* and *pbpA* is similar to that of an MreC depletion strain (Wei *et al*., 2003; Leaver and Errington, 2005). This suggested that MreC and the two PBPs act in the same pathway of cylindrical cell wall synthesis. Moreover, affinity purification using *C. crescentus* extracts showed that MreC interacts with several PBPs (Divakaruni *et al*., 2005). We therefore decided to test whether *B. subtilis* MreC interacted directly with various PBPs. Full-length MreC gave a posi-

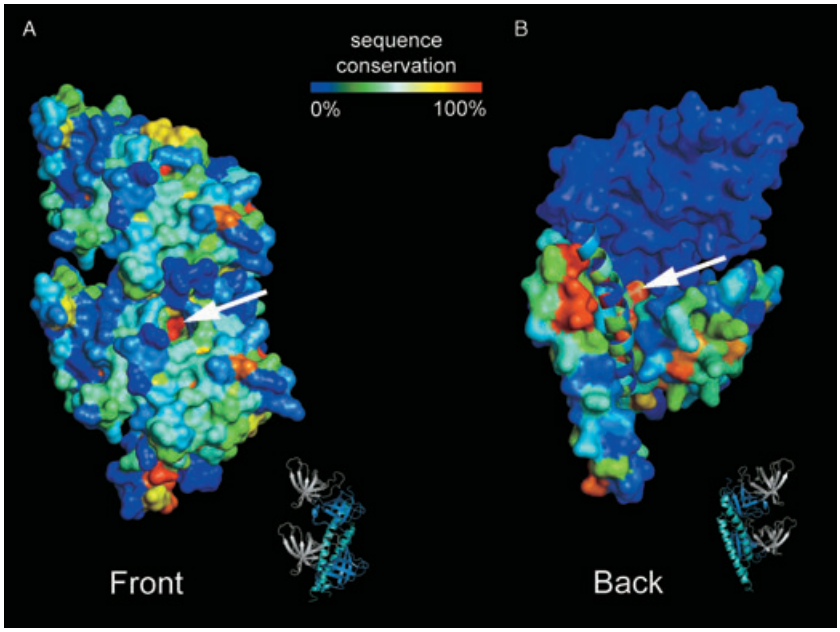

Fig. 4. Conservation plot of MreC dimer. Based on an alignment of over 30 different *mreC* genes the degree of conservation of each residue was calculated and plotted onto the surface of the structure of the MreC dimer. A mini-ribbon plot is added to facilitate orientation of the molecule (with colour code as in Fig. 1A).
A. MreC dimer from the front, arrow pointing into the tunnel towards the conserved Ser residue. Highly conserved residues are in red, least conserved residues in blue.
B. MreC dimer 180° rotated along the *y*-axis. To facilitate discrimination between the two monomers, one of them is depicted in blue. The N-terminal helix of this monomer, shown in ribbon representation, blocks access to the conserved diad (arrow) upon dimerization.

tive two-hybrid signal for those PBPs that belong to class A and class B high-molecular-weight PBPs (PBP2b, PBP1, PBP2a, PBP3, PBP4, PBP2c, PBP2d, PbpH and PBP4b), but not for the low-molecular-weight peptidases (PBP4*, PBP5*, PbpX and PBP5; Fig. 6, Table 1). The low-molecular-weight carboxypeptidase, PBP4a, showed weak interaction with MreC (Fig. 6, Table 1). This supports a model in which MreC modulates cylindrical cell wall synthesis via the murein synthases, rather than the hydrolases. As quiet a number of the high-molecular-weight PBPs interact with MreC it is plausible that MreC might have a PBP recognition sequence that establishes the interaction. Most of the interactions between MreC and the PBPs required the β-domains of MreC (PBP1, PBP2a, PBP3 PBP4, PBP2c and PBP4b; Fig. 6). However, the N-terminal domain of MreC, including the periplasmic and transmembrane helices, seemed to be sufficient for interaction with PBP2b, PBP2d and perhaps PbpH (Fig. 6). As reported previously, the helical localization of MreC might or might not be dependent on the MreB cytoskeleton (Figge *et al*., 2004; Divakaruni *et al*., 2005; Dye *et al*., 2005; Kruse *et al*., 2005; Leaver and Errington, 2005). The sequence of the cytoplasmic tail of MreC is quite variable and is very short in some organisms (only six aa residues in *B. subtilis*), so it seems unlikely that this makes a strong interaction with MreB. Possibly, the third protein encoded by the *mre* operon, MreD, could function as an intermediate, establishing the link between the cytoplasmic MreB cytoskeleton and MreC. Quantification of the abundance of *B. subtilis* MreC by Western blotting showed that it is present at about 12 000 molecules (monomers) per cell (Fig. 5C), similar to the values reported previously for Mbl (12 000–14 000) and MreB (8000) (Jones *et al*., 2001). This high abundance suggests that MreC may have a structural, rather than an enzymatic role in cell wall synthesis, and in principle, it could make a structure on the outside of the cytoplasmic membrane that follows the MreB/Mbl helix along its entire length. This structure, together with MreD might act as a scaffold to which high-molecular-weight PBPs are recruited in order to spatially organize the synthesis of new cell wall material to maintain the rod shape of the cell.

Experimental procedures

MreC protein expression and purification

The gene encoding MreC (NCBI Accession No. CAC99625; TrEMBL Q8Y6Y4) was amplified from *L. monocotogenes* genomic DNA (ATCC 19115D) by PCR starting from the codon for amino acid 50. The PCR product, generated with the forward primer (5′-CTTTAAGAAGGAGATATACATAT GAATATAGTAGCTAAGCCTACTTCAT) and reverse primer (5′-AATGATGATGATGATGATGGGATCCTTGGCCTCCAGT CGTGTCTGAACTA), was used as a primer pair to insert the gene into vector pHis17 (B. Miroux, pers. comm.) according to a restriction-free cloning procedure as described previously (van den Ent and Löwe, 2006). The newly obtained plasmid, pFE164, contains the *mreC* gene downstream of the T7 promoter, encoding the periplasmic part of MreC with a His-tag at the C-terminus to facilitate purification. In the same way, the periplasmic domain of *E. coli* MreC and *B. subtilis* MreC were cloned, resulting in plasmids pFE147 (*B. subtilis* MreC starting from aa 50) and pFE150 (*E. coli* MreC starting from aa 57).

MreC was expressed in Bl21AI cells (Invitrogen) at 25°C and purified using Histrap HP (Amersham) affinity purification at pH 6.0, essentially as described before (van den Ent and Löwe, 2000). After the protein was eluted from the column it

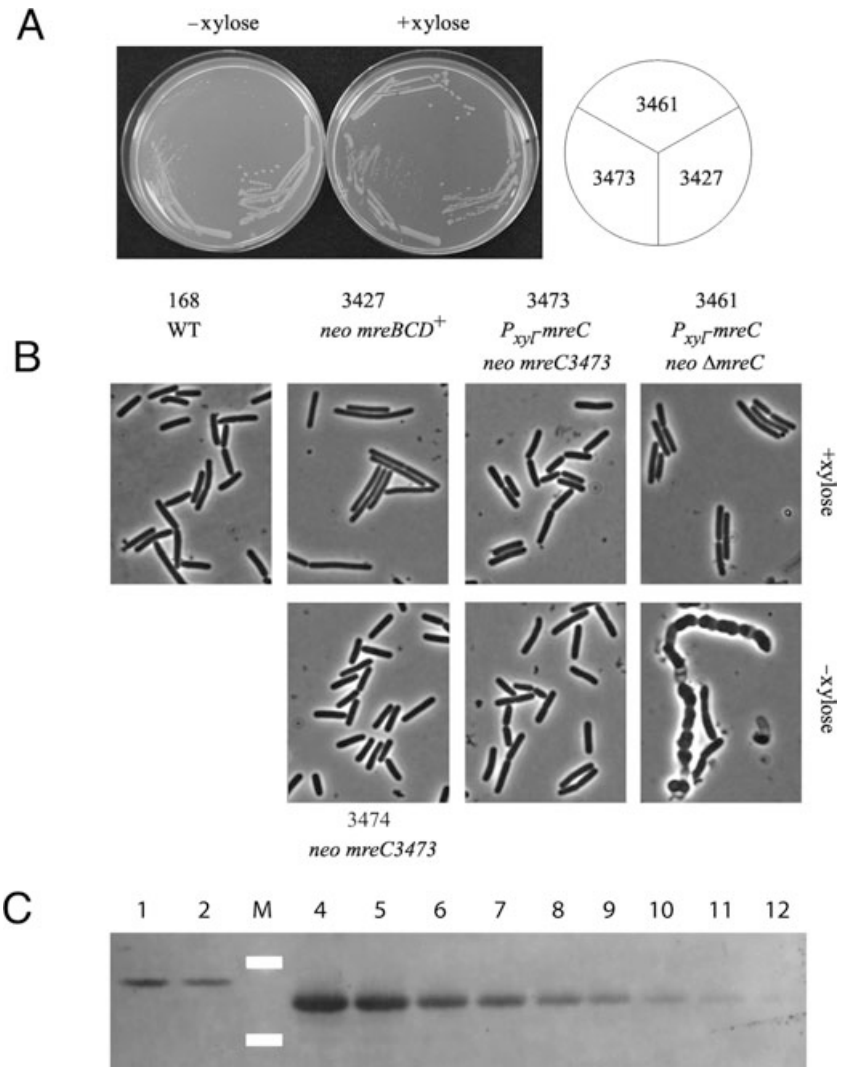

Fig. 5. A. Strains 3427 (*neo mreB*+), 3473 [*amyE*::(*spc* P_{xyl}-*mreC*) *neo mreB*$^{+}$*mreC*^{TS230AA}] and 3461 [*amyE*::(*spc* P_{xyl}-*mreC*) *neo mreB*$^{+}$ Δ*mreC*] were grown overnight at 37°C on nutrient agar with and without 0.5% xylose. Cells of strain 168 (wild-type *B. subtilis*) are shown for comparison.
B. Images of strains from (A) grown at 37°C in CH medium with and without 0.5% xylose.
C. Western blot quantifying the total number of MreC molecules per cell in *B. subtilis*. Total cell lysate diluted twofold (loaded approximately 6.7×10^7 and 3.35×10^7 cells per lane (lanes 1 and 2) and pure MreC protein (periplasmic domain, from *B. subtilis*) with a concentration of 105 to 0.5 ng (lanes 4–12). Lane 3 (M) shows markers of 33 and 48 kDa.

was concentrated by ultrafiltration using vivaspin 10 k MWCO (Vivascience) and loaded onto a size-exclusion column Sephacryl S200 in TEN7.0 (20 mM Tris 7.0, 1 mM EDTA, 1 mM NaAzide). Typically, yields were around 18 mg from 1 l of culture for *L. monocytogenes* MreC. Selenomethionine-containing MreC was expressed in Bl21AI cells, which is non-auxotrophic for methionine. By using specific growth conditions methionine biosynthesis was inhibited (Van Duyne *et al*., 1993). A pre-culture, grown in 2× TY, was used in a 1:1000 dilution to inoculate 200 ml of minimal medium containing 1× M9 supplemented with 0.4% glucose, 2 mM $MgSO_4$, 100 μg ml^{-1} ampicillin, 1 μg ml^{-1} of each of the vitamins (riboflavin, niacinamide, pyrodoxine, thiamine), and 1:100 diluted Trace elements (1 l Trace elements contains 50 g of EDTA, 0.8 g of $FeCl_3 \cdot 6H_2O$, 0.05 g of $ZnCl_2$, 0.01 g of $CuCl_2$, 0.01 g of $CoCl_2 \cdot 6H_2O$, 0.01 g of H_3BO_3, 1.6 g of $MnCl_2$, 0.01 g of $NiSO_4$, 0.01 g of molybdic acid, adjusted to pH 7.0). The overnight culture was diluted 1:50 into 10 l of minimal medium and grown for 4 h to optical density at 600 nm (OD_{600}) of 0.30 at 36°C, when the temperature was dropped to 25°C. Once the OD_{600} reached a value of 0.5 a mixture of L-amino acids was added as solids [per litre of culture: 50 mg of selenomethionine (Acros), 50 mg of leucine, isoleucine, valine and 100 mg of lysine, threonine and phenylalanine (all from Fluka)]. After 15 min, protein expression was induced by the addition of 0.2% arabinose and the culture was grown for an additional 9 h. Protein purification was performed as described for the non-substituted protein, except that 5 mM β-mercaptoethanol was added to the buffers for the Ni^{2+} column and 5 mM dithiothreitol (DTT) was used in all other buffers. A typical yield was 2.5 mg of protein per litre of cells. Electrospray mass spectrometry measurements of the non-substituted protein and the selenomethionine-containing protein was used to check selenomethionine incorporation, indicating that all five methionines were substituted by selenomethionine (MreC observed 27 587.0 Da, calculated 27 589.0 Da; SeMet MreC observed 27 822.0 Da; calculated 27 822.0 Da).

Crystallization and structure determination

MreC was crystallized at 86 mg ml^{-1} by sitting-drop vapour diffusion in 17.7% ethanol, 100 mM Bis-Tris-Propane, pH 7.1

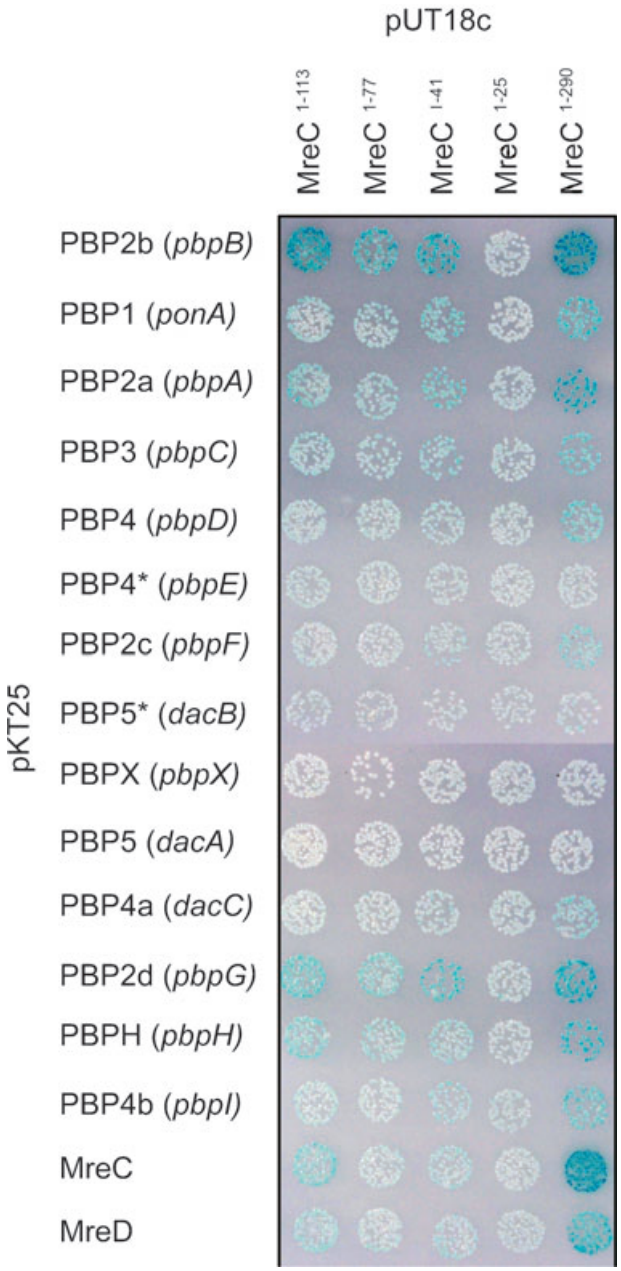

Fig. 6. Bacterial two-hybrid data on the interactions between deletion mutants of MreC and PBPs as well as MreD. Strains of *E. coli BTH101* expressing truncations of MreC from plasmid pUT18c and either of the PBPs from pKT25 were spotted onto minimal media supplemented with X-gal and incubated at 30°C until a blue colour developed. The results are from a single experiment performed on the same day with strains spotted on one plate.

and the crystals were flash frozen in liquid nitrogen in the presence of 18.7% ethanol, 15% glycerol and 100 mM Bis-Tris-Propane 7.1. Selenomethionine substituted MreC crystallized in 14.4% ethanol and 100 mM ADA 6.0 and the crystals were flash frozen in 17% ethanol, 15% glycerol and 100 mM ADA 6.0. MreC crystals belong to space group P622 with two molecules in the asymetric unit. Cell constants were a = 162.95 Å, b = 162.95 Å, c = 95.39 Å (Table 2). Data sets were collected at beamlines SRS 10.1 (Cianci *et al.*, 2005) (selenomethionine containing crystals) and ESRF ID29 (native data set).

All data were indexed and integrated with MOSFLM (Leslie, 1991) and further processed using the CCP4 package (Collaborative Computing Project, 1994). An initial electron density map was generated with the MAD data using SOLVE (Terwilliger and Berendzen, 1999) and phases were calculated with SHARP (de la Fortelle and Bricogne, 1997). The model was built manually with the program MAIN (Turk, 1992) and refined using CNS (Brünger *et al.*, 1998). Details of the refined model are shown in Table 3.

Construction of a strain of B. subtilis *expressing MreC^{TS229AA}*

The Thr229 and Ser230 codons of the *B. subtilis mreC* gene were mutated into alanines. As MreC is an essential gene (Lee and Stewart, 2003; Leaver and Errington, 2005) these residues were mutated at the chromosomal locus in a strain with an ectopic copy of *mreC* at the *amyE* locus under the control of the P_{xyl} promoter. The mutation was introduced by linkage to a *neo* cassette that conveys resistance to kanamycin. To do this we utilized strain 3427 (*trpC2 Ωneo3427*; Leaver and Errington, 2005), which contains a neomycin cassette upstream the promoter of *mreB*. Chromosomal DNA of this strain was used to PCR amplify segments of DNA that contained the *neo* cassette and the *mreBCD* operon with the desired mutation in *mreC*. Two primers (USF5, TCCTGGTATGCAGGCCTGTT and USF3, TGCT TCAATAAGATCGCCTTTTT mutation indicated) were designed to amplify a fragment of DNA stretching from 3 kb upstream of the neomycin marker to the codon for the threonine residue at position 229 which was mutated to an alanine

Table 1. MreC interactions.

Protein	Gene	PBP class[a]	MreC[b]
PBP1	*ponA*	HMW class A	++
PBP4	*pbpD*	HMW class A	++
PBP2c	*pbpF*	HMW class A	+
PBP2d	*pbpG*	HMW class A	+++
PBP2b	*pbpB*	HMW class B	+++
PBP2a	*pbpA*	HMW class B	+++
PBP3	*pbpC*	HMW class B	++
PbpH	*pbpH*	HMW class B	+++
PBP4b	*pbpI*	HMW class B	++
PBP4a	*dacC*	LMW carboxypeptidase	+
PBP4*	*pbpE*	LMW endopeptidase	–
PBP5*	*dacB*	LMW carboxypeptidase	–
PbpX	*pbpX*	LMW endopeptidase	–
PBP5	*dacA*	LMW carboxypeptidase	–
MreC	*mreC*		+++
MreD	*mreD*		+++

a. PBP, penicillin binding protein. HMW: high-molecular-weight PBPs are either class A with transpeptidase and transglycosylase activities or class B with transpeptidase activity. LMW: low-molecular-weight PBPs are either carboxypeptidases or endopeptidases.
b. MreC: interaction with full-length MreC as determined in bacterial two-hybrid screen (scoring: –, no interaction; + to +++, weak to strong interaction, based on Fig. 6).

Table 2. Crystallographic data.

P622:	a = 162.95 Å, b = 162.95 Å, c = 95.39 Å				
Crystal	l (Å)	Resol. (Å)	I/sI[a]	Rm[b]	Multipl.[c]
PEAK	0.9802	3.0	22.9 (6.3)	0.089	10.2
INFL	0.9804	3.0	17.3 (3.9)	0.128	10.2
HREM	0.9766	3.0	21.0 (5.2)	0.101	10.1
NATI	0.9792	2.5	9.8 (1.9)	0.100	3.4

a. Signal to noise ratio of intensities, highest resolution bin in brackets.
b. R_m: $S_hS_i|I(h, i) - I(h)|/S_hS_i\ I(h, i)$ where I(h, i) are symmetry-related intensities and I(h) is the mean intensity of the reflection with unique index h.
c. Multiplicity for unique reflections, for MAD data sets I(+) and I(–) are kept separate.

codon by the 3′ primer USF3. Two more primers (DSF3, CCAGCACCCGAGCAGCAGGC and DSF5, GCAGGGA CAGGCGGTGTTTT CCC) were designed to amplify a fragment stretching from the serine residue at position 230, which was mutated to code for an alanine by the 5′ primer DSF5, and extending 3 kb downstream of the *mreC* stop codon. Primers USF3 and DSF5 were phosphorylated with polynucleotide kinase (Roche) and used with primers USF5 and DSF3 to PCR amplify fragments of DNA from chromosomal DNA of strain 3427. These two fragments where then purified, ligated together and used to transform competent cells of strain 3437, which contains an ectopic copy of *mreC* at the *amyE* locus. The resulting strain, 3473, had the mutated form of *mreC* at the chromosomal locus (designated allele *mreC3473*), which was complemented by the wild-type copy of *mreC* at *amyE*. The genotype of this strain was confirmed by PCR and sequencing of the whole *mreBCD* operon. In order to separate the mutant *mreC* allele from the ectopic copy, wild-type *B. subtilis* was transformed with chromosomal DNA of strain 3473 and selected for kanamycin. Strains were isolated that were kanamycin resistant and spectinomycin sensitive, indicating that they had not inherited the ectopic copy of *mreC*. Analysis by PCR and digestion showed that four out of five strains had the *mreC3473* allele. The presence of the mutation was verified by sequence analysis (strain 3474).

Table 3. Refinement statistics.

	NATI
Residues	1: 74–283; 2: 77–277
Resolution	2.5 Å
R-factor, R-free[a]	0.245, 0.266
B average[b]	75.6 Å^2
Geometry bonds/angles[c]	0.009 Å, 1.469°
Ramachandran[d]	86.9%/0.0%
PDB ID[e]	2j5u, r2j5usf

a. Five per cent of reflections were randomly selected for determination of the free R-factor, prior to any refinement.
b. Temperature factors averaged for all atoms.
c. RMS deviations from ideal geometry for bond lengths and restraint angles (Engh and Huber, 1991).
d. Percentage of residues in the 'most favoured region' of the Ramachandran plot and percentage of outliers (PROCHECK; Laskowski *et al*., 1993).
e. Protein Data Bank identifiers for co-ordinates and structure factors respectively.

Growth and maintenance of B. subtilis *strains*

For growth experiments, *B. subtilis* strains were grown at 37°C in CH media (Partridge and Errington, 1993), supplemented with or without xylose. *B. subtilis* cells were transformed by the method of Kunst and Rapoport (1995), then plated onto nutrient agar (Oxoid) supplemented with 5 μg ml^{-1} kanamycin with 0.5% xylose. To screen transformants, colonies were patched onto nutrient agar containing 50 μg ml^{-1} spectinomycin with 0.5% xylose.

Quantitative Western

The number of MreC molecules per cell was determined by quantitative Western analysis. The quantity of protein from total cell extract was compared with a dilution series of purified protein. Rabbit antiserum was raised against MreC from *B. subtilis* (periplasmic part aa 50–290) using a commercial service provided by Eurogentec. Wild-type *B. subtilis* was grown in CH media to an OD_{600} of approximately 0.8 and the number of cells per OD unit was determined using a haemocytometer. Two dilutions of total cell lysate and a dilution series of pure MreC protein were separated by electrophoresis on a 4–12% Bis-Tris midi gel (Invitrogen) before being transferred to polyvinylidene difluoride membrane for 3.5 h at 20 mAmps using a wet transfer apparatus (Trans-Blot^{TM}Cell, Bio-Rad). The membrane was blocked with 4% milk powder in PBS before being incubated with a 1:10 000 dilution of anti-MreC antiserum then a 1:10 000 dilution of anti-rabbit IgG conjugated to horseradish peroxidase (Sigma). The antibody was detected using an ECL+ kit (Amersham Biosciences) and the membrane was scanned on an FLA-5000 fluoroimager (Fuji). The protein concentration of the total cell lysate was estimated by comparing the fluorescence intensities of bands on the scanned membrane to those of the standard protein using the Aida Image Analyser program (Raytest).

Construction of a strain of E. coli *expressing MreC^{TS222AA}*

The Thr222 and Ser223 codons of the *E. coli mreC* gene were mutated to encode Ala222 and Ala223 using the Quikchange site-directed mutagenesis method (Stratagene). Briefly, plasmid pFB211[*lacI*^{q} P_{lac}::*mreC-rfp*] was used as a template for temperature-cycled amplification with primers designed to introduce mutations into both codons. Amplifica-

tion was carried out with KOD polymerase (Novagen) and primers 5′-GGTGATGTGCTGGTTGCGGCCGGTCTGGGC GGTCGTTTCC-3′ and 5′-GGAAA CGACCGCCCAGACC GGCCGCAACCAGCACATCACC-3′ (alanine codons underlined). The product was treated with DpnI to digest unamplified DNA and transformed into competent DH5α cells. The resulting plasmid (pFB218) contained the desired mutations as verified by sequence analysis.

Construction of a truncated MreC protein encoding amino acids 1 through 104 fused to RFP was made as follows. The *mreC* reading frame from *E. coli* MG1655 chromosomal DNA was amplified by PCR with primers 5′-CTAGTC TAGAATACGAGAATACGCATAACTT-3′ and 5′-CCGCTCG AGCAGCGGGGAACCCAGCAG*CTCG*-3′. The product was digested with XbaI and XhoI (sites underlined). Unexpectedly, the product contained an additional XhoI site near the 3′ primer annealing site (beginning of site is in italics) leading to a slightly shorter fragment than anticipated. The 339 bp fragment was used to replace the 1143 XbaI–XhoI fragment of pFB211, yielding pFB223[P_{lac}::*mreC*(1–104)-*rfp*].

Construction of plasmids pFB112, pFB128 and pFB211, and of strain FB15 will be detailed elsewhere (F. Bendezu and P. de Boer, in preparation).

Bacterial two hybrid

We used the bacterial two-hybrid system developed by Karimova *et al*. (1998). Full-length and truncated versions of the *mreC* gene were amplified by PCR and ligated into the pKT25 vector. All the other constructs carrying MreD and PBP fusions were derived from plasmid pUT18c (M. Leaver, R. Daniel and J. Errington, in preparation). Half microlitre of pUT18c derivative and 0.5 μl of pKT25 derivative was added to a pre-chilled 0.5 ml tube with 20 μl of *E. coli* BTH101 competent cells and incubated at 4°C for 30 min. Cells were then heat shocked at 42°C for 90 s. One hundred and eighty microlitres of 2× TY supplemented with 20 mM glucose was added and cells were allowed to recover at 30°C for 45 min before being spotted onto minimal media agar plates with 0.5 mM IPTG. Minimal medium was made up of A+B (3.6 μM $FeCl_3 \cdot 6H_2O$, 40 μM $MgCl_2 \cdot 6H_2O$, 0.1 mM $MnCl_2 \cdot 4H_2O$, 10 mM NH_4Cl, 75 μM Na_2SO_4, 0.5 mM KH_2PO_4, 1.2 mM NH_4NO_3) supplemented with 1 mM $MgSO_4$, 0.8% glucose, 0.0001% thiamine, 0.2% casine hydrolysate (Oxoid), 0.008% X-gal [form a 4% stock in dimethylformamide (BDH)], 100 μg ml^{-1} ampicillin, 25 μg ml^{-1} kanamycin, and solidified with 1.5% bacteriological agar (agar number 1, Oxoid). Plates were incubated at 30°C for 24–48 h, and any colour change was noted.

Acknowledgements

This work was supported by a Human Frontier Science Program Award (RGP0001-C103) to J.L., P.d.B. and J.E. F.B. was also supported by NIH NRSA Institutional Training Grant T32GM08056. ML was supported by an MRC Graduate Studentship. We would like to thank Dr R. Daniel for his help and stimulating discussions during the course of this work and are grateful to Dr M. Cianci for his support while beamline SRS 10.1 (Daresbury, UK) was commissioned.

References

Amos, L.A., van den Ent, F., and Löwe, J. (2004) Structural/functional homology between the bacterial and eukaryotic cytoskeletons. *Curr Opin Cell Biol* **16:** 24–31.

Barton, G.J. (1993) ALSCRIPT: a tool to format multiple sequence alignments. *Protein Eng* **6:** 37–40.

Bhavsar, A.P., and Brown, E.D. (2006) Cell wall assembly in *Bacillus subtilis*: how spirals and spaces challenge paradigms. *Mol Microbiol* **60:** 1077–1090.

Brünger, A., Adams, P.D., Clore, G.M., DeLano, W.L., Gros, P., Grosse-Kunstleve, R.W., *et al.* (1998) Crystallography & NMR system: a new software suite for macromolecular structure determination. *Acta Crystallogr D Biol Crystallogr* **54:** 905–921.

Carballido-Lopez, R., and Errington, J. (2003) The bacterial cytoskeleton: *in vivo* dynamics of the actin-like protein Mbl of *Bacillus subtilis*. *Dev Cell* **4:** 19–28.

Carballido-López, R., Formstone, A., Li, Y., Ehrlich, S.D., Noirot, P., and Errington, J. (2006) Actin homologue MreBH governs cell morphogenesis by localization of the cell wall hydrolase LytE. *Dev Cell* **11:** 399–409.

Cianci, M., Antonyuk, S., Bliss, N., Bailey, M.W., Buffey, S.G., Cheung, K.C., *et al.* (2005) A high-throughput structural biology/proteomics beamline at the SRS on a new multipole wiggler. *J Synchrotron Radiat* **12:** 455–466.

Collaborative Computing Project, N. (1994) The CCP4 suite: programs for protein crystallography. *Acta Crystallogr D* **50:** 760–763.

Daniel, R.A., and Errington, J. (2003) Control of cell morphogenesis in bacteria: two distinct ways to make a rod-shaped cell. *Cell* **113:** 767–776.

de la Fortelle, E., and Bricogne, G. (1997) Maximum-likelihood heavy-atom parameter refinement for multiple isomorphous replacement and multiwavelength anomalous diffraction methods. In *Methods in Enzymology: Macromolecular Crystallography, Part A*, Vol. 276. Sweet, R.M., and Carter, C.W., Jr (eds). New York, NY: Academic Press, pp. 472–494.

Defeu Soufo, H.J., and Graumann, P.L. (2004) Dynamic movement of actin-like proteins within bacterial cells. *EMBO Rep* **5:** 789–794.

DeLano, W.L. (2002) *The PYMOL Molecular Graphics System*. San Carlos, CA: DeLano Scientific.

Divakaruni, A.V., Loo, R.R., Xie, Y., Loo, J.A., and Gober, J.W. (2005) The cell-shape protein MreC interacts with extracytoplasmic proteins including cell wall assembly complexes in *Caulobacter crescentus*. *Proc Natl Acad Sci USA* **102:** 18602–18607.

Dye, N.A., Pincus, Z., Theriot, J.A., Shapiro, L., and Gitai, Z. (2005) Two independent spiral structures control cell shape in *Caulobacter*. *Proc Natl Acad Sci USA* **102:** 18608–18613.

Engh, R.A., and Huber, R. (1991) Accurate bond and angle parameters for x-ray protein-structure refinement. *Acta Crystallogr A* **47:** 392–400.

van den Ent, F., and Löwe, J. (2000) Crystal structure of the cell division protein FtsA from *Thermotoga maritima*. *EMBO J* **19:** 5300–5307.

van den Ent, F., and Löwe, J. (2006) RF cloning: a restriction-free method for inserting target genes into plasmids. *J Biochem Biophys Meth* **67:** 67–74.

van den Ent, F., Amos, L.A., and Löwe, J. (2001) Prokaryotic origin of the actin cytoskeleton. *Nature* **413:** 39–44.

Figge, R.M., Divakaruni, A.V., and Gober, J.W. (2004) MreB, the cell shape-determining bacterial actin homologue, co-ordinates cell wall morphogenesis in *Caulobacter crescentus*. *Mol Microbiol* **51:** 1321–1332.

Formstone, A., and Errington, J. (2005) A magnesium-dependent *mreB* null mutant: implications for the role of *mreB* in *Bacillus subtilis*. *Mol Microbiol* **55:** 1646–1657.

Fuhrmann, C.N., Kelch, B.A., Ota, N., and Agard, D.A. (2004) The 0.83 A resolution crystal structure of alpha-lytic protease reveals the detailed structure of the active site and identifies a source of conformational strain. *J Mol Biol* **338:** 999–1013.

Gitai, Z., Dye, N., and Shapiro, L. (2004) An actin-like gene can determine cell polarity in bacteria. *Proc Natl Acad Sci USA* **101:** 8643–8648.

Gitai, Z., Dye, N.A., Reisenauer, A., Wachi, M., and Shapiro, L. (2005) MreB actin-mediated segregation of a specific region of a bacterial chromosome. *Cell* **120:** 329–341.

Heidrich, C., Ursinus, A., Berger, J., Schwarz, H., and Höltje, J.V. (2002) Effects of multiple deletions of murein hydrolases on viability, septum cleavage, and sensitivity to large toxic molecules in *Escherichia coli*. *J Bacteriology* **184:** 6093–6099.

Henriques, A.O., Glaser, P., Piggot, P.J., and Moran, C.P., Jr (1998) Control of cell shape and elongation by the rodA gene in *Bacillus subtilis*. *Mol Microbiol* **28:** 235–247.

Holm, L., and Sander, C. (1993) Protein-structure comparison by alignment of distance matrices. *J Mol Biology* **233:** 123–138.

Höltje, J.V. (1998) Growth of the stress-bearing and shape-maintaining murein sacculus of *Escherichia coli*. *Microbiol Mol Biol Rev* **62:** 181–203.

Jones, L.J.F., Carballido-Lopez, R., and Errington, J. (2001) Control of cell shape in bacteria: helical, actin-like filaments in *Bacillus subtilis*. *Cell* **104:** 913–922.

Karimova, G., Pidoux, J., Ullmann, A., and Ladant, D. (1998) A bacterial two-hybrid system based on a reconstituted signal transduction pathway. *Proc Natl Acad Sci USA* **95:** 5752–5756.

Kraulis, P.J. (1991) MOLSCRIPT: a program to produce both detailed and schematic plots of protein structures. *J Appl Crystallogr* **24:** 946–950.

Kruse, T., and Gerdes, K. (2005) Bacterial DNA segregation by the actin-like MreB protein. *Trends Cell Biol* **15:** 343–345.

Kruse, T., Moller-Jensen, J., Lobner-Olesen, A., and Gerdes, K. (2003) Dysfunctional MreB inhibits chromosome segregation in *Escherichia coli*. *EMBO J* **22:** 5283–5292.

Kruse, T., Bork-Jensen, J., and Gerdes, K. (2005) The morphogenetic MreBCD proteins of *Escherichia coli* form an essential membrane-bound complex. *Mol Microbiol* **55:** 78–89.

Kruse, T., Blagoev, B., Lobner-Olesen, A., Wachi, M., Sasaki, K., Iwai, N., *et al.* (2006) Actin homolog MreB and RNA polymerase interact and are both required for chromosome segregation in *Escherichia coli*. *Genes Dev* **20:** 113–124.

Kunst, F., and Rapoport, G. (1995) Salt stress is an environmental signal affecting degradative enzyme synthesis in *Bacillus subtilis*. *J Bacteriol* **177:** 2403–2407.

Laskowski, R.A., MacArthur, M.W., Moss, D.S., and Thornton, J.M. (1993) Procheck – a program to check the stereochemical quality of protein structures. *J Appl Crystallogr* **26:** 283–291.

Leaver, M., and Errington, J. (2005) Roles for MreC and MreD proteins in helical growth of the cylindrical cell wall in *Bacillus subtilis*. *Mol Microbiol* **57:** 1196–1209.

Lee, J.C., and Stewart, G.C. (2003) Essential nature of the *mreC* determinant of *Bacillus subtilis*. *J Bacteriol* **185:** 4490–4498.

Lee, J.C., Cha, J.H., Zerbv, D.B., and Stewart, G.C. (2003) Heterospecific expression of the *Bacillus subtilis* cell shape determination genes *mreBCD* in *Escherichia coli*. *Curr Microbiol* **47:** 146–152.

Leslie, A.G.W. (1991) *Recent Changes to the MOSFLM Package for Processing Film and Image Plate Data*. Daresbury, Warrington WA44AD, UK: SERC Laboratory.

Levin, P.A., Margolis, P.S., Setlow, P., Losick, R., and Sun, D.X. (1992) Identification of *Bacillus subtilis* genes for septum placement and shape determination. *J Bacteriol* **174:** 6717–6728.

Löwe, J., van den Ent, F., and Amos, L.A. (2004) Molecules of the bacterial cytoskeleton. *Annu Rev Biophys Biomol Struct* **33:** 177–198.

Merritt, E.A., and Bacon, D.J. (1997) Raster3D: photorealistic molecular graphics. In *Methods in Enzymology: Macromolecular Crystallography, Part B*, Vol. 277. Carter, C.W., and Sweet, R.M. (eds). London: Academic Press, pp. 505–524.

Nelson, D.E., and Young, K.D. (2000) Penicillin binding protein 5 affects cell diameter, contour, and morphology of *Escherichia coli*. *J Bacteriol* **182:** 1714–1721.

Nilsen, T., Ghosh, A.S., Goldberg, M.B., and Young, K.D. (2004) Branching sites and morphological abnormalities behave as ectopic poles in shape-defective *Escherichia coli*. *Mol Microbiol* **52:** 1045–1054.

Partridge, S.R., and Errington, J. (1993) The importance of morphological events and intercellular interactions in the regulation of prespore-specific gene expression during sporulation in *Bacillus subtilis*. *Mol Microbiol* **8:** 945–955.

Popham, D.L., and Young, K.D. (2003) Role of penicillin-binding proteins in bacterial cell morphogenesis. *Curr Opin Microbiol* **6:** 594–599.

Rashid, R., Liang, B., Baker, D.L., Youssef, O.A., He, Y., Phipps, K., *et al.* (2006) Crystal structure of a Cbf5-Nop10-Gar1 complex and implications in RNA-guided pseudouridylation and dyskeratosis congenita. *Mol Cell* **21:** 249–260.

Slovak, P.M., Porter, S.L., and Armitage, J.P. (2006) Differential localization of Mre proteins with PBP2 in *Rhodobacter sphaeroides*. *J Bacteriol* **188:** 1691–1700.

Soufo, H.J., and Graumann, P.L. (2003) Actin-like proteins MreB and Mbl from *Bacillus subtilis* are required for bipolar positioning of replication origins. *Curr Biol* **13:** 1916–1920.

Spratt, B.G. (1975) Distinct penicillin binding proteins involved in the division, elongation, and shape of *Escherichia coli K12*. *Proc Natl Acad Sci USA* **72:** 2999–3003.

Spratt, B.G., and Pardee, A.B. (1975) Penicillin-binding proteins and cell shape in *E. coli*. *Nature* **254:** 516–517.

Tamaki, S., Matsuzawa, H., and Matsuhashi, M. (1980) Cluster of *mrdA* and *mrdB* genes responsible for the rod

shape and mecillinam sensitivity of *Escherichia coli*. *J Bacteriol* **141:** 52–57.

Terwilliger, T.C., and Berendzen, J. (1999) Automated MAD and MIR structure solution. *Acta Crystallogr D Biol Crystallogr* **55:** 849–861.

Tiyanont, K., Doan, T., Lazarus, M.B., Fang, X., Rudner, D.Z., and Walker, S. (2006) Imaging peptidoglycan biosynthesis in *Bacillus subtilis* with fluorescent antibiotics. *Proc Natl Acad Sci USA* **103:** 11033–11038.

Turk, D. (1992) *Weiterentwicklung eines Programms für Molekülgrafik und Elektrondichte-Manipulation und seine Anwendung auf verschiedene Protein-Strukturaufklärungen*. PhD Thesis. Technische Universität München.

Van Duyne, G.D., Standaert, R.F., Karplus, P.A., Schreiber, S.L., and Clardy, J. (1993) Atomic structures of the human immunophilin Fkbp-12 complexes with Fk506 and rapamycin. *J Mol Biol* **229:** 105–124.

Varley, A.W., and Stewart, G.C. (1992) The Divivb region of the *Bacillus subtilis* chromosome encodes homologs of *Escherichia coli* septum placement (Mincd) and cell-shape (Mrebcd) determinants. *J Bacteriol* **174:** 6729–6742.

Wachi, M., Doi, M., Tamaki, S., Park, W., Nakajima-Iijima, S., and Matsuhashi, M. (1987) Mutant isolation and molecular cloning of *mre* genes, which determine cell shape, sensitivity to mecillinam, and amount of penicillin-binding proteins in *Escherichia coli*. *J Bacteriol* **169:** 4935–4940.

Wachi, M., Doi, M., Okada, Y., and Matsuhashi, M. (1989) New *mre* genes *mreC* and *mreD*, responsible for formation of the rod shape of *Escherichia coli* cells. *J Bacteriol* **171:** 6511–6516.

Wei, Y., Havasy, T., McPherson, D.C., and Popham, D.L. (2003) Rod shape determination by the *Bacillus subtilis* class B penicillin-binding proteins encoded by pbpA and pbpH. *J Bacteriol* **185:** 4717–4726.